SCIENCE CHINA
Life Sciences

•RESEARCH PAPER•

https://doi.org/10.1007/s11427-022-2166-y

An antibody cocktail with broadened mutational resistance and effective protection against SARS-CoV-2

Chunyun Sun[1†], Hang Chi[2†], Fei Yuan[3†], Jing Li[1], Ji Yang[1], Aihua Zheng[3], Fei Wang[1], Lingling Sun[1], Yanjing Zhang[1], Ping Hu[1], Lihua Jiao[1], Yongqiang Deng[2*] & Liangzhi Xie[1,4,5*]

[1]*Beijing Engineering Research Center of Protein and Antibody, Sinocelltech Ltd., Beijing 100176, China;*
[2]*Department of Virology, State Key Laboratory of Pathogen and Biosecurity, Beijing Institute of Microbiology and Epidemiology, Academy of Military Medical Sciences, Beijing 100071, China;*
[3]*State Key Laboratory of Integrated Management of Pest Insects and Rodents, Institute of Zoology, Chinese Academy of Sciences, Beijing 100101, China;*
[4]*Beijing Key Laboratory of Monoclonal Antibody Research and Development, Sino Biological Inc., Beijing 100176, China;*
[5]*Cell Culture Engineering Center, Chinese Academy of Medical Sciences & Peking Union Medical College, Beijing 100005, China*

Received May 23, 2022; accepted July 20, 2022; published online September 29, 2022

Neutralizing antibodies have been proven to be highly effective in treating mild and moderate COVID-19 patients, but continuous emergence of SARS-CoV-2 variants poses significant challenges. Antibody cocktail treatments reduce the risk of escape mutants and resistance. In this study, a new cocktail composed of two highly potent neutralizing antibodies (HB27 and H89Y) was developed, whose binding epitope is different from those cocktails that received emergency use authorization. This cocktail showed more potent and balanced neutralizing activities (IC_{50} 0.9–11.3 ng mL^{-1}) against a broad spectrum of SARS-CoV-2 variants over individual HB27 or H89Y antibodies. Furthermore, the cocktail conferred more effective protection against the SARS-CoV-2 Beta variant in an aged murine model than monotherapy. It was shown to prevent SARS-CoV-2 mutational escape *in vitro* and effectively neutralize 61 types of pseudoviruses harbouring single amino acid mutation originated from variants and escape strains of Bamlanivimab, Casirivimab and Imdevimab with IC_{50} of 0.6–65 ng mL^{-1}. Despite its breadth of variant neutralization, the HB27+H89Y combo and EUA cocktails lost their potencies against Omicron variant. Our results provide important insights that new antibody cocktails covering different epitopes are valuable tools to counter virus mutation and escape, highlighting the need to search for more conserved epitopes to combat Omicron.

SARS-CoV-2, COVID-19, epitopes, antibody cocktail, mutational escape

Citation: Sun, C., Chi, H., Yuan, F., Li, J., Yang, J., Zheng, A., Wang, F., Sun, L., Zhang, Y., Hu, P., et al. (2022). An antibody cocktail with broadened mutational resistance and effective protection against SARS-CoV-2. Sci China Life Sci 65, https://doi.org/10.1007/s11427-022-2166-y

INTRODUCTION

The global COVID-19 pandemic caused by the severe acute respiratory syndrome coronavirus 2 (SARS-CoV-2) infection has led to severe public health burden and socioeconomic crises (WHO, 2022). Therapeutic antibodies targeting the receptor binding domain (RBD) of the spike protein have been developed based on the prototype strain, and some of which have been authorized for emergency use in prophylaxis and treatment of COVID-19 (Du et al., 2021; Lu et al., 2020; Sadoff et al., 2021). However, since the initial report of the genome of the prototype SARS-CoV-2 strain (Wuhan-Hu-1, MN908947.3), several new mutations in the spike (S) protein have been reported, including B.1.1.7 (Alpha), B.1.351 (Beta), B.1.617.2 (Delta) and B.1.1.529 (Omicron)

†Contributed equally to this work
*Corresponding authors (Liangzhi Xie, email: LX@sinocelltech.com; Yongqiang Deng, email: dengyq1977@126.com)

which has contributed to several waves of worldwide pandemic infections (Burki, 2021; Chen et al., 2020; Deng et al., 2021; Liu et al., 2021; Plante et al., 2021; Tao et al., 2021; Zhou et al., 2022). Unfortunately, the fast mutation rate in the RBD region has led to antibody evasion, which hinders the effectiveness of therapeutic antibodies against upcoming variants.

Antibody cocktails are comprised of two or more monoclonal antibodies against different epitopes on the target-of-interest (S protein for COVID-19). They are efficacious treatment regimens for COVID-19 and are regarded as more resistant to antibody evasion due to the coverage of multiple epitopes (Baum et al., 2020; Weisblum et al., 2020). Examples of current COVID-19 therapeutic antibody cocktails include Casirivimab (REGN10933) and Imdevimab (REGN10987), Bamlanivimab (LY-CoV555) and Etesevimab (LY-CoV016), as well as Tixagevimab (AZD8895) and Cilgavimab (AZD1061). The Casirivimab and Imdevimab cocktail has been authorized for treatment of mild to moderate patients infected by SARS-CoV-2 variants Alpha, Beta, Gamma, or Delta (FDA, 2022a); Bamlanivimab and Etesevimab cocktail has been authorized for treating patients infected by SARS-CoV-2 variants Alpha and Delta (FDA, 2022b). Recent reports indicates variants containing RBD substitutions such as K417N/T, E484K, N501Y, and L452R have been shown to escape from neutralization by one of the monoclonal antibodies in the cocktails (Starr et al., 2021; Tada et al., 2022).

An alternative approach to prevent mutation-mediated antibody escape is the identification of "broad-spectrum" antibodies. Recently, a monoclonal antibody, sotrovimab (derived from S309 (Pinto et al., 2020)), was authorized for emergency use for the treatment of COVID-19. Sotrovimab maintained a moderate neutralizing activity against all VOCs except Omicron BA.2 (Takashita et al., 2022a; Takashita et al., 2022b). Structural analysis revealed that the epitope of sotrovimab was a non-angiotensin-converting enzyme 2 (ACE2) binding region within the RBD which interacted partially with RBD epitope site IV (Piccoli et al., 2020).

The above neutralizing antibodies covered a variety of epitopes and possessed different neutralizing activities to various variants. To date, there has neither been antibody cocktail nor broad-spectrum antibody that has shown to be fully immune to mutation-mediated antibody escape. All things considered, the development of new antibody cocktails covering different epitopes could provide additional treatment options for COVID-19.

HB27 is an IgG1 neutralizing antibody with the "LALA" modification in the Fc region to diminish interaction with Fc receptors and complement. HB27 is highly potent with a 50% plaque reduction neutralization value ($PRNT_{50}$) of 0.22 nmol L^{-1} *in vitro* and highly efficacious with >99.9% reduction in lung viral load in a mouse challenging model (Zhu et al., 2021). Phase I clinical trial (NCT04483375) showed HB27 was well-tolerated in healthy participants even at maximum dose of 50 mg kg^{-1} and had nearly linear dose-proportional pharmacokinetics (PK) parameters (Li et al., 2021a; Li et al., 2021b). Two adaptive phase II/III trials have been initiated in high risk COVID-19 outpatients (NCT04709328) and in hospitalized COVID-19 patients (NCT04644185).

In this study, a new antibody cocktail with two highly potent neutralizing antibodies, HB27 and H89Y, was evaluated to verify the extent of its neutralizing activities against SARS-CoV-2 variants, in comparison with the two individual antibodies and EUA cocktails.

RESULTS

H89Y does not compete with HB27 for binding to prototype RBD

Antibody cocktail is a promising approach to increase the therapeutic efficacy and reduce risks of mutation-mediated antibody escape by emerging SARS-CoV-2 variants (FDA, 2022b). To identify another antibody suitable for cocktail combination with HB27, a panel of SARS-CoV-2 specific antibodies was screened by phage display to identify candidates that could bind to RBD not competitively with HB27 in ELISA (Figure S1 in Supporting Information). A highly potent neutralizing antibody H89Y was identified as a suitable candidate for cocktail combination with HB27 (Figure S2 in Supporting Information). H89Y is a humanized immunoglobulin (IgG) which originated from mouse antibody using conventional CDR grafting method. H89Y bound to RBD and Spike with a similar binding affinity as compared to HB27 (Figure S3 in Supporting Information) and exerted pM affinity against prototype RBD (K_D=6.8 pM) and spike (K_D=22 pM) (Figure 1A and B). RBD binding features of HB27 and H89Y were characterized in a sequential bio-layer interferometry (BLI) assay, confirming that H89Y co-bound to RBD and spike protein with HB27 (Figure 1C, Table S1 in Supporting Information).

Epitope analysis of H89Y and the H89Y+HB27 cocktail

To further characterize the critical RBD residues for H89Y binding, a library of recombinant prototype RBD variants containing mutations within or around the ACE2 binding sites were utilized for a deep mutation scan. Each RBD variant was individually expressed in HEK293 cells and its binding against H89Y was determined (Figure 2A). The results showed that RBD residues G476, S477, P479, F486, N487, and Y489 were the key binding sites for H89Y. Mutations of these residues (G476D, S477I, F486S and N487R) completely abolished H89Y binding while P479Y and

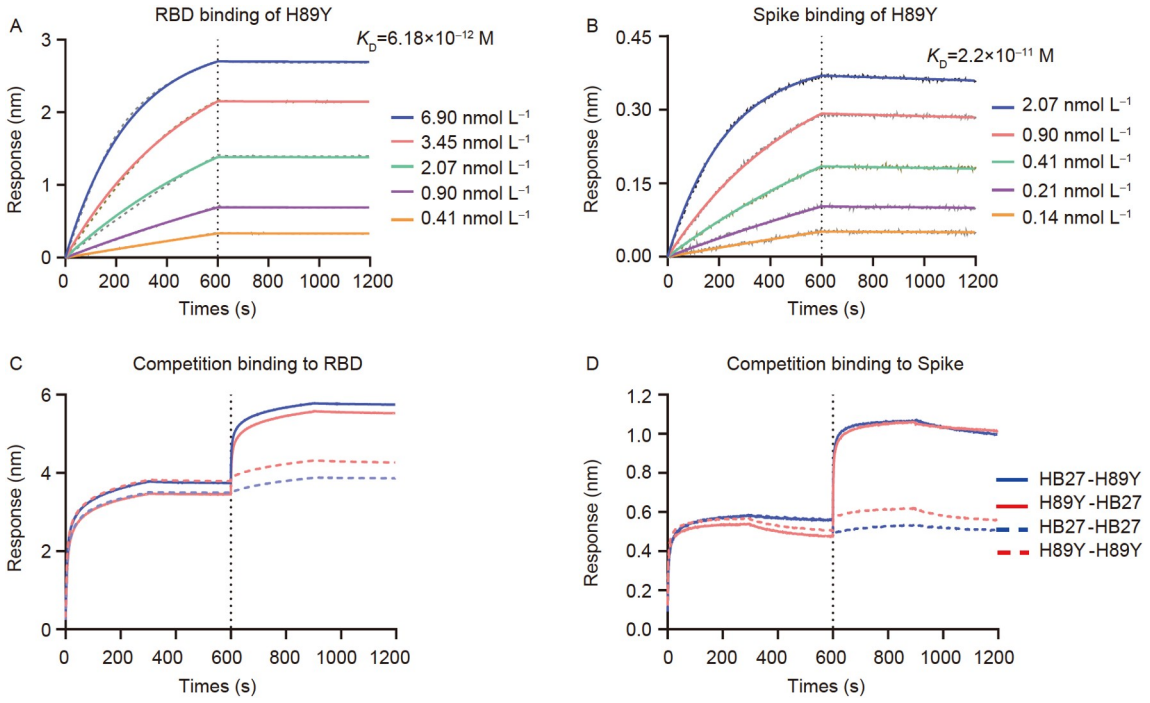

Figure 1 Identification of H89Y as the pairing candidate with HB27 for antibody cocktail. Binding kinetics of H89Y to recombinant prototype RBD (A) or spike (B) protein measured by BLI. The equilibrium dissociation constants (K_D) were labelled in each graph. The vertical dashed lines indicated the boundaries of the association and dissociation phases. C, Competitive binding of HB27 and H89Y to recombinant prototype RBD and spike protein evaluated by BLI. Sample loading sequences were labelled as antibody 1-antibody 2. The vertical dashed lines indicated the time for loading of the second antibody in each assay.

Y489R substitutions sharply reduced H89Y-RBD interactions. These residues constituted the epitope of H89Y. Amino acid residues, including T478 E484, F490 and Q474, also seemed to contribute to the H89Y binding, but to a lesser degree. The corresponding single mutations of T478 E484, F490 and Q474 resulted in a <50% decrease of H89Y-RBD binding as compared to the wild type (WT) counterpart. Structural analysis showed that these amino acid residues were all located in the RBM region while residues G476, S477, F486, N487, Y489 and E484 were directly involved with ACE2 interactions (Figure 2B and C), suggesting molecular mechanism for SARS-CoV-2 neutralization by H89Y was through blocking ACE2-spike binding.

H89Y bound to RBD in a non-overlapping region distant from the epitope of HB27 (Zhu et al., 2021). Co-binding of HB27 and H89Y blocked the ACE2-spike interaction (Figure 2B and C). The combined binding footprint of HB27+H89Y cocktail on RBD was apparently different from those of the other antibody cocktails such as Imdevimab+Casirivimab (Hansen et al., 2020), Bamlanivimab (Jones et al., 2021) +Etesevimab (Shi et al., 2020), as well as Tixagevimab +Cilgavimab (Zost et al., 2020) (Figure 2D–F). Among these neutralizing antibodies (nAb), Imdevimab, Casirivimab, Etesevimab, Tixagevimab and HB27 bound to site Ia in RBD, Bamlanivimab and Cilgavimab interacted with site Ib (Corti et al., 2021), while H89Y bound to the site between Ia/Ib.

The HB27+H89Y cocktail effectively neutralizes various SARS-CoV-2 pseudovirus and authentic virus

Firstly, we characterized the binding potency of the HB27 +H89Y antibody cocktail against the prototype strain. The antibody cocktail interacted with recombinant RBD (K_D=7.8 pM, Figure 3A) and spike proteins (K_D=92 pM, Figure 3B) with high affinities. In comparison to HB27 or H89Y alone, the cocktail showed comparable blocking curves in ACE2-RBD and ACE2-spike protein competitive ELISA assays (Figure 3C). We also tested the neutralizing activities of the HB27 +H89Y cocktail as well as the two individual antibodies against several current and previous variant of concern (VOC), variant of interest (VOI) strains using the PsV assay (Figure 3D, Table 1). Both HB27 and H89Y showed high potency in neutralizing the D614G strain with the IC_{50} values of 2.2–3.0 ng mL^{-1}. But for variants, HB27 showed 11-fold higher bioactivity against Delta than the H89Y antibody, while H89Y was more potent than HB27 in neutralizing against the other variants, especially the Alpha, Beta, and Mu variant. As expected, the cocktail showed a clear advantage over either individual antibody, with potent and balanced neutralizing activities (IC_{50} 0.9–11.3 ng mL^{-1}) against a broader spectrum of SARS-CoV-2 variants.

In comparison with Imdevimab+Casirivimab and Bamlanivimab+Etesevimab cocktails, the HB27+H89Y cocktail exhibited relatively higher neutralization potency against

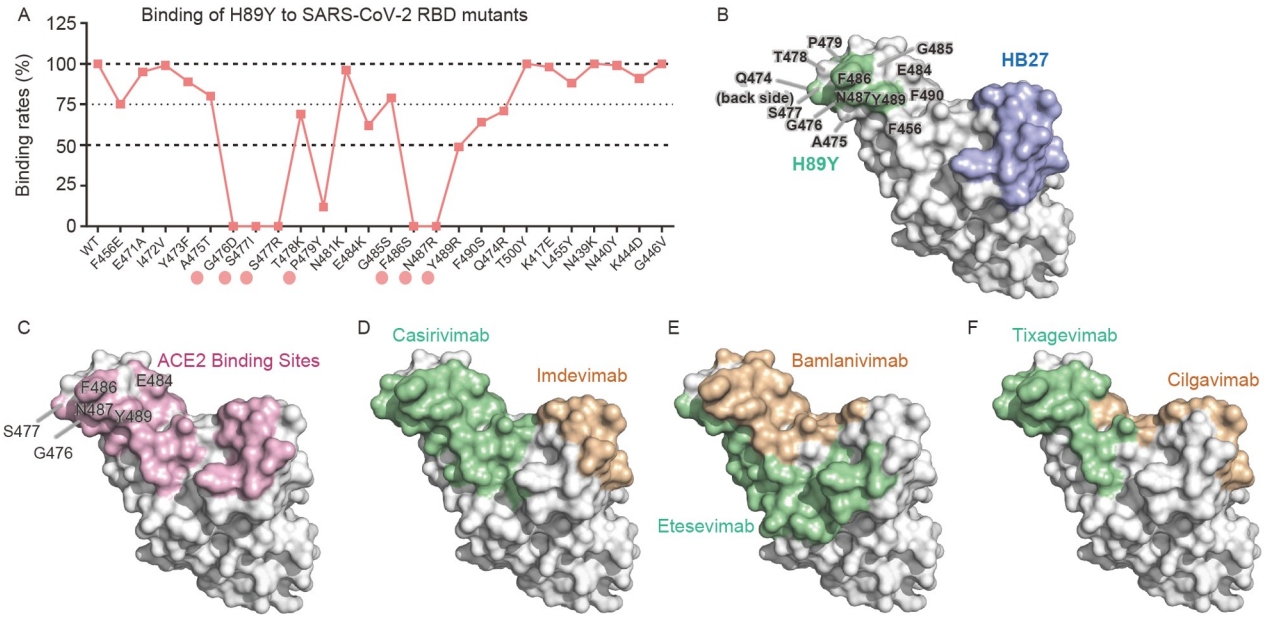

Figure 2 Epitope mapping of H89Y. A, Recombinant prototype RBD mutants were used for key residues mapping for H89Y. Mutations that led to over 50% decrease of binding compared with the WT RBD were identified as critical binding sites. Mutations that led to less than 50% but over 25% reduction of binding compared with the WT RBD protein were identified as possible binding sites. B, The epitopes of H89Y and HB27. RBD was shown in surface model. The critical binding sites of H89Y identified by mutational analysis were colored in green and residues contributed to H89Y binding to a lesser degree were also labelled. The epitope of HB27 was colored in blue according to its cryo-electron microscopy structure (PDB: 7CYP). C, ACE2 binding area on RBD was colored pink (PDB: 6LZG) and shared residues in RBD interacting to both H89Y and ACE2 were labelled. Binding epitopes of EUA antibody cocktails in RBD, including the Imdevimab and Casirivimab cocktail (D, PDB: 6XDG), the Bamlanivimab and Etesevimab cocktail (E, PDB: 7KMG and 7C01), and the Tixagevimab and Cilgavimab cocktail (F, PDB: 7L7E).

both prototype strain PsV with IC_{50} of 3.4 ng mL^{-1} (Figure 4A) and authentic viral strains of prototype, Beta and Delta variants (IC_{50}=49, 49 and 146 ng mL^{-1}, respectively) in a micro-neutralization test (MNT) (Figure 4B).

Protective efficacy of the HB27+H89Y cocktail against SARS-CoV-2 Beta variant in aged BALB/c mice

Aged BALB/c mice (7–8 months old) were intranasally challenged with 4×10^5 PFU mL^{-1} authentic SARS-CoV-2 Beta variant (CSTR.16698.06.NPRC 2.062100001) (Chen et al., 2022; Gu et al., 2020). Mice were randomized into 4 groups: four in the PBS control group, three in 400 μg of HB27 monotherapy group, three in 400 μg of H89Y monotherapy group, and five in 400 μg of HB27 and 400 μg of H89Y cocktail group. The number of mice in each group was not even due to BSL-3 capacity. Four hours after virus inoculation, the tested mice were injected intravenously with either PBS or antibody (Figure 5A). The viral load in lung tissues of control mice at five days post infection (5 dpi) was 9.5 log_{10}RNA copies g^{-1}. Compared with control group, viral load in lung tissues was reduced by 353-folds to 6.9 log_{10}RNA copies g^{-1} (*, P=0.0298) in the HB27 monotherapy group, and by 951-folds to 6.5 log_{10}RNA copies g^{-1} (****, P<0.0001) in the H89Y monotherapy group. The HB27+H89Y cocktail treatment resulted in a more significant 31989-fold viral load reduction to 5.0 log_{10}RNA copies g^{-1} (***, P=0.0004) (Figure 5B). In addition, histological results showed that control mice exhibited moderate to severe interstitial pneumonia with remarkably increased thickness of the alveolar septum, inflammatory cells infiltration, and congested blood vessels. Either individual antibodies or the cocktail, significantly alleviated lung damage at 5 dpi with only mild lesions of alveolar epithelial cells, focal hemorrhage and inflammatory cell infiltration (Figure 5C). These results suggested that HB27 or H89Y antibody as monotherapy was highly effective in treating SARS-CoV-2 Beta variant infection in aged mice, while the HB27+H89Y cocktail was even more efficacious in reducing viral load.

The HB27+H89Y cocktail prevents mutational escape from individual antibodies

A replication-competent vesicular stomatitis virus (VSV) recombinant expressing GFP reporter and SARS-CoV-2 spike protein (rVSV-eGFP-SARS-CoV-2) was employed to test the HB27+H89Y cocktail in preventing mutational escape (Baum et al., 2020; Li et al., 2020; Li et al., 2021a). rVSV-eGFP-SARS-CoV-2 was passed on Vero cells in the presence of various concentrations of individual antibody or antibody cocktail for 4 days. The supernatant of the wells containing the greatest antibody concentrations in passage 1

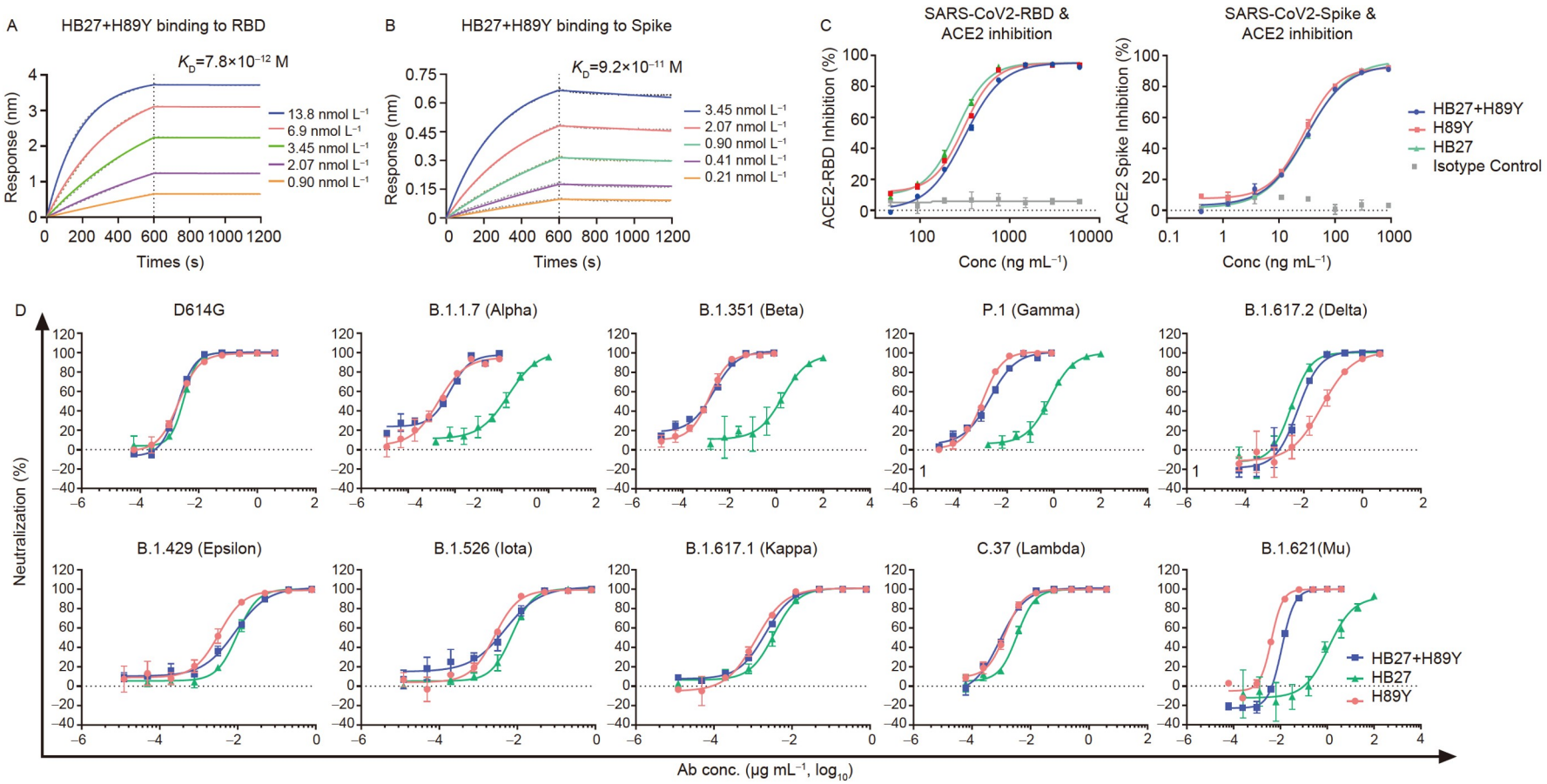

Figure 3 HB27+H89Y cocktail potent binds, blocks and neutralizes SARS-CoV-2. Binding kinetics of the HB27 and H89Y cocktail to recombinant prototype RBD (A) or spike (B) protein measured by BLI. K_Ds were labelled in each graph. The vertical dashed lines indicated the boundaries of the association and dissociation phases. C, Dose-dependent blocking of prototype RBD and spike binding to ACE2 by individual HB27, H89Y and the HB27 and H89Y cocktail. The Isotype control is a non-spike targeting IgG1 antibody with LALA mutation in Fc. D, PsV neutralization against the SARS-COV-2 D614G and variant strains in Huh-7 cells.

Table 1 Neutralizing potency (IC_{50}, ng mL^{-1}) of HB27, H89Y and HB27+H89Y cocktail against VOC, VOI strains

WHO Name	Strain	HB27	H89Y	HB27+H89Y	Fold Improvement of Cocktail*
D614G	D614G	3.0	2.2	1.8	1.7
Alpha	B.1.1.7	1944.0	2.0	6.3	308.6
Beta	B.1.351	1874.0	1.4	2.1	892.4
Gamma	P.1	678.1	0.9	1.9	356.9
Delta	B.1.617.2	3.7	41.5	6.3	6.6#
Epsilon	B.1.429	9.7	3.3	8.6	1.1
Iota	B.1.526	7.3	2.6	4.9	1.5
Kappa	B.1.617.1	3.5	1.2	2.1	1.7
Lambda	C.37	3.5	1.4	0.9	3.9
Mu	B.1.621	1154.0	4.1	11.3	102.1

* Fold bioactivity improvement of cocktail over the weaker individual HB27 except # (H89Y) antibody calculated by dividing the higher IC_{50} values of HB27 or H89Y by the IC_{50} value of the cocktail.

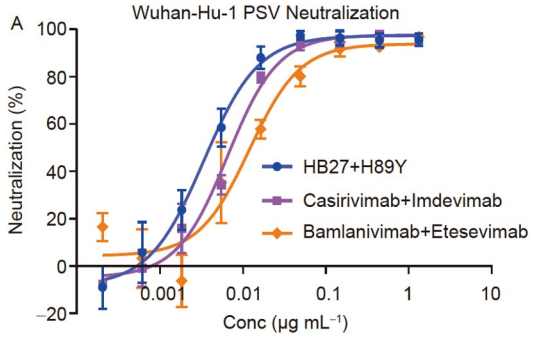

B

Virus strain	Authentic virus neutralizing IC_{50} ng mL^{-1}		
	HB27+H89Y	Casirivimab +Imdevimab	Bamlanivimab +Etesevimab
Prototype	49	98	293
Beta	49	293	3125
Delta	146	195	1172

Figure 4 HB27+H89Y cocktail potent neutralizes SARS-CoV-2 compared with EUA antibody cocktails. A, Neutralization of the HB27+H89Y cocktail, Imdevimab+Casirivimab cocktail and Bamlanivimab+Etesevimab cocktail against prototype PsV (Wuhan-Hu-1) in Huh-7 cells. B, Authentic virus neutralizing potency of the HB27 and H89Y cocktail against prototype, Beta and Delta virus compared with Imdevimab+Casirivimab and Bamlanivimab +Etesevimab cocktails.

(P1) with extensive GFP-positive foci were collected and underwent the second round selection (Figure 6A). After two rounds, the escape mutants that occurred in each group were analyzed using next generation sequencing (NGS) of the S gene (Table S2 in Supporting Information). Three mutations, including P499S in the HB27 treated samples and S477F or F486S in the H89Y treated samples were identified. On the other hand, no escape mutations were observed in the RBD region after two rounds of screening under the selective pressure of the HB27+H89Y cocktail. As expected, pseudoviruses carrying these mutations were resistant to the treatment of corresponding antibodies as shown by the drastic loss of neutralizing activity but not sensitive to the other antibody or the antibody cocktail (Figure 6B and Table 2).

The HB27+H89Y cocktail showed broad neutralizing activities against SARS-CoV-2 variants

61 types of prototype PsVs with single amino acid mutations were constructed for neutralizing assays to test resistance to HB27, H89Y and the HB27+H89Y cocktail (Table 3). These single mutations were originated from pandemic strains and resistant strains against EUA antibodies (FDA, 2022a; FDA, 2022b). The antibody cocktail showed consistently high neutralizing activities to all 61 types of pseudoviruses, while significant changes in bioactivities against some mutants were observed with one of the two antibodies, further illustrating the significant advantages and importance of the antibody cocktail in coping with rapid virus mutation.

Antibody evasion from omicron variant

The Omicron variant contains massive mutation sites in RBD that leads to antibody evasion and significant loss of vaccine efficacy (Cao et al., 2022a; Cao et al., 2022b; Dejnirattisai et al., 2022b; Liu et al., 2022; Takashita et al., 2022a; Tseng et al., 2022). The HB27+H89Y cocktail along with three EUA SARS-CoV-2 nAb cocktails were assessed in PsV assays against Delta and Omicron sub-lineage BA.1. In comparison to the potent neutralizing activities against Delta variant, these cocktails showed complete loss or a 390-

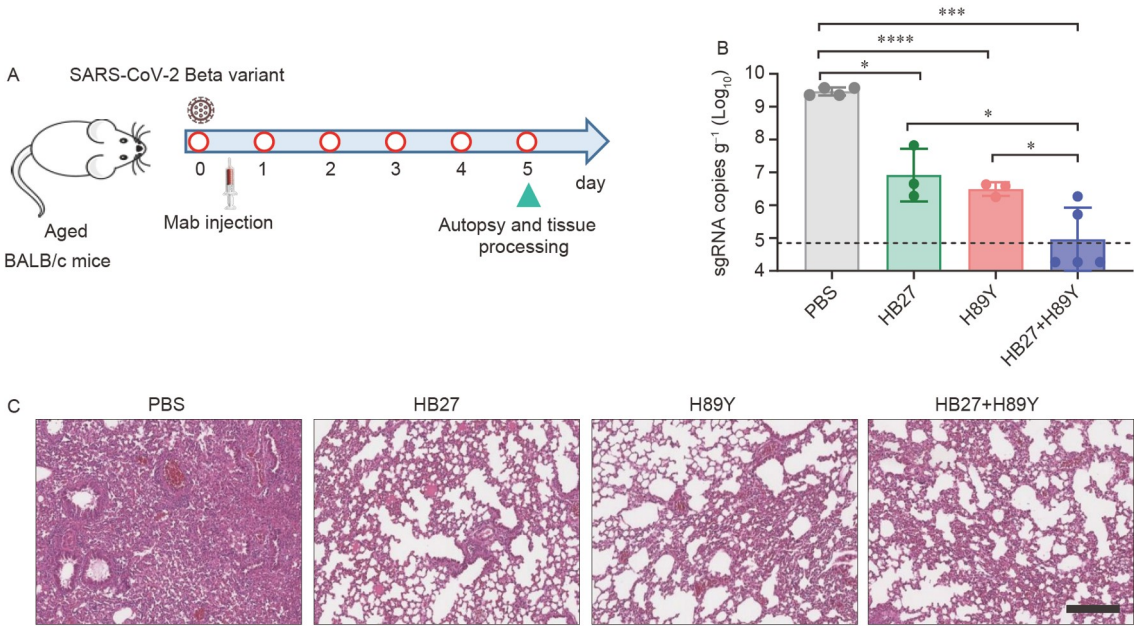

Figure 5 Protective efficacy of HB27, H89Y and cocktail against SARS-CoV-2 Beta variant in aged BALB/c mice. A, Schematic representation of the virus challenge study. Aged BALB/c mice were intranasally challenged with the SARS-CoV-2 Beta (CSTR.16698.06.NPRC 2.062100001) variant. Four hours after virus infection, mice were injected intravenously with vehicle PBS or antibodies (N=4/3/3/5). Mice were sacrificed for autopsy and tissue processing at 5 dpi. B, Viral load of subgenomic (sg) RNA in the lung tissue was measured in each group. C, H & E staining was used for observation of damage in the lung tissues of mice in each group. Comparison was made between groups and performed by two-tailed unpaired test and Welch's t-test. *, $P \leq 0.0394$, ***, P=0.0004, ****, $P \leq 0.0001$ were considered statistically significant. Individual animal values were indicated by colored symbols. Scale bar: 200 μm.

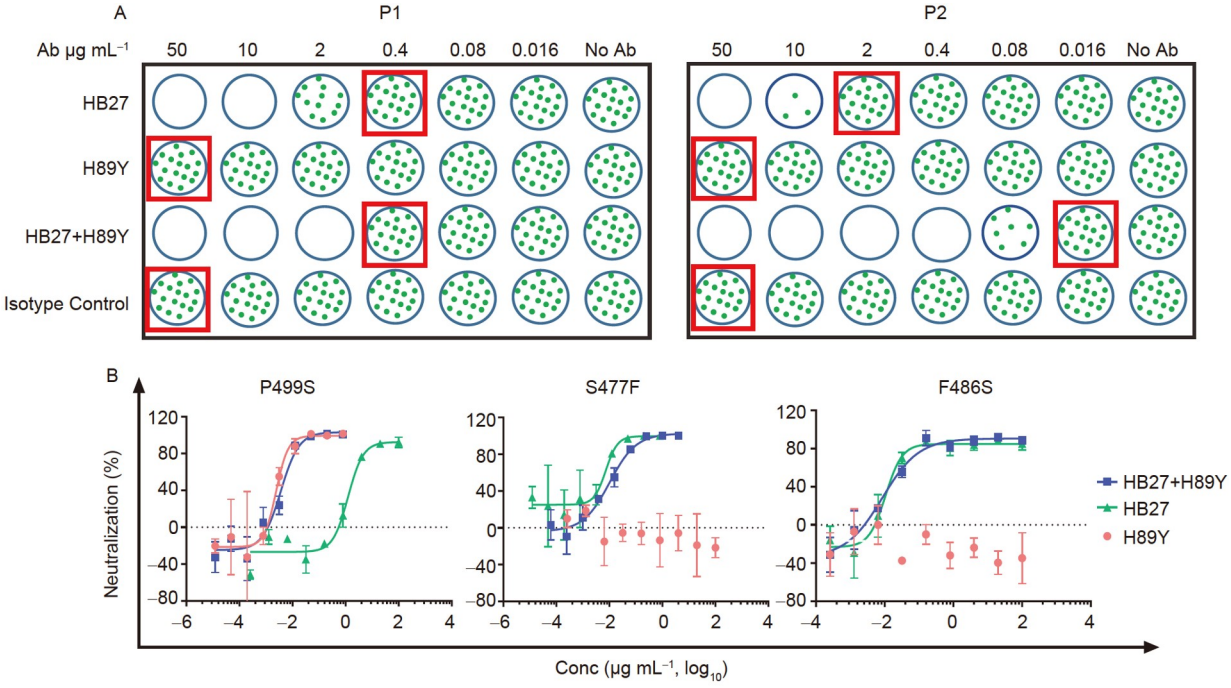

Figure 6 Escape mutation screening for HB27, H89Y and the antibody cocktail. A, The diagram of two rounds (P1 and P2) of escape mutant selection using rVSV-eGFP-SARS-CoV-2. The supernatants from the wells (red squares) containing the highest antibody concentrations that showed extensive GFP signals were passed and/or sequenced. An isotype antibody underwent the same selection to monitor for tissue culture adaptations. B, Neutralization IC_{50} curves agasint PsV carrying the spike with amino acid substitutions identified from GFP positive samples by NGS analysis.

fold reduction (Tixagevimab+Cilgavimab) in neutralizing activity against Omicron sub-lineage BA.1 (Figure 7A). K417N, G446S, E484A or Q493R substitutions in Omicron sub-lineage BA.1 caused complete or partial loss of neutralization of those EUA antibody cocktails (Tada et al., 2022). Among the nine PsVs carrying spike with single

Table 2 Neutralizing potency (IC_{50}, ng mL^{-1}) against PsV carrying escape mutations

mAb	Mutant	PSV neutralizing		
		HB27	H89Y	HB27+H89Y
HB27	P499S	1238	2.4	3.6
H89Y	S477F	7.3	–	10.2
	F486S	10.6	–	8.5
HB27+H89Y	NA	/	/	/

NA, not applicable. "/", not determined. "–", the neutralizing activity of the antibody was insufficient for IC_{50} curve fitting.

amino acid substitution in RBD of omicron BA.1 variant, neutralizing capabilities of HB27 and H89Y were obviously affected by N501Y and S477N substitution respectively with the activities decreasing over 476.0 and 272.9 fold compared to that of D614G strain (Figure 7B, Table 3). These results provided the possible explanation for extensive escape from Omicron variant of HB27+H89Y.

DISCUSSION

Following the emergence of the SARS-CoV-2 virus in 2019, there have been unending reports of viral mutations—a catalyst for the series of COVID-19 waves so far. Recent reports indicate mutations in the RBD region of spike protein resulted in significant reductions in monoclonal antibody potency and vaccine efficacy (Andrews et al., 2022; Liu et al., 2021; Takashita et al., 2022a; Takashita et al., 2022b; Tseng et al., 2022). As a countermeasure, combination of two or multiple neutralizing antibodies as cocktails have been developed and shown to be efficacious in treating COVID-19 in clinic (FDA, 2022a; FDA, 2022b). In spite of the unpredictable nature of high viral replication driving the mutations, there is no denying that cocktails may perform differently against the new variants. Thus, new antibody cocktails covering epitopes different from the EUA cocktails could offer additional treatment options to combat future variants.

In this study, we identified two highly potent neutralizing antibodies, HB27 and H89Y that recognized non-overlapping RBD epitopes (HB27 bound to site Ia in RBD (Zhu et al., 2021) while H89Y interacted with site Ia/b). These epitopes were different from those of Casirivimab+Imdevimab, Etesevimab+Bamlanivimab, as well as Tixagevimab+Cilgavimab (Figure 2). As expected, compared with the single antibody, the HB27+H89Y cocktail showed a different escape resistance spectrum against the highly mutated SARS-CoV-2 and exhibited potent inhibition activities against all pandemic VOC and VOI variants prior to the emergence of Omicron (Figure 3, Tables 1 and 3). The HB27+H89Y cocktail was shown to be more potent than the Casirivimab+Imdevimab and Etesevimab+Bamlanivimab cocktails in PsV and authentic virus neutralization assays (Figure 4). In addition, the cocktail also demonstrated potent and broad spectrum of neutralizing activities against 61 types of pseudoviruses bearing a variety of single site mutations from variants and escape strains of Bamlanivimab, Casirivimab and Imdevimab. However, significant losses of neutralizing potencies were observed with the two individual antibodies against some pseudoviruses (Table 3).

The advantages of the cocktail over single component antibodies were further demonstrated in a mutation escape experiment. After two passages of the pseudovirus in cell culture, the cocktail showed negative in the mutational escape occurrence as compared to HB27 or H89Y antibody alone (Figure 6 and Table 2). Similarly, clinical trial results of the Etesevimab+Bamlanivimab cocktail also showed lower frequency of mutations in the combo group than those in the two single antibody groups (FDA, 2020). In SARS-CoV-2 Beta variant protection efficacy study carried out in aged mice, the cocktail treatment reduced viral load by 31989-fold from the untreated control mice vs. 353-fold and 951-fold viral load reductions in the two single antibody treatment groups of HB27 and H89Y, respectively (Figure 5).

In a previously published paper, the HB27 antibody showed *in vivo* protection against a SARS-CoV-2 prototype virus (BetaCoV/Beijing/IME-BJ01/2020) in an ACE2 humanized mouse model and a SARS-CoV-2 mouse adaptive strain (MASCp6) in a BALB/c mouse model (Zhu et al., 2021). The HB27+H89Y antibody cocktail showed an improved *in vivo* efficacy against Beta variant in comparison to HB27 and H89Y antibodies as monotherapies in this study. Due to BSL-3 capacity limitation, no further *in vivo* challenging studies were carried out with the HB27 and H89Y cocktail.

Liang et al. (2021) showed that the neutralization of SARS-CoV-2 antibody *in vitro* correlated with its protective efficacy *in vivo*. Upon neutralization data to a newly emerged variant, US FDA has authorized treatments of COVID-19 patients infected with new variants with EUA antibodies approved on the basis of clinical efficacy against earlier SARS-CoV-2 strains, without repeating *in vivo* challenging studies or new clinical trials. The HB27+H89Y antibody cocktail showed potent and balanced neutralizing activities against a wide range of variants (Figures 3 and 4, Tables 1 and 3), as well as a distinct characteristic of preventing SARS-CoV-2 escape mutation (Figure 6), and hence is expected to have strong protective efficacies against most of the VOC variants *in vivo*.

Despite the high neutralizing activities of the two cocktail components, as well as the cocktail's balanced neutralization against a broad spectrum of variants and antibody resistant strains, large number of mutations in the RBD regions of new Omicron escaped. Clear indication of antibody evasion observed for the Omicron variant was explained by the neu-

Table 3 Neutralizing potency (IC_{50}, ng mL^{-1}) against a panel of SARS-CoV-2 prototype PsVs carrying single-site mutations

Mutations in RBD	Variant Strains	Mutation Type	HB27	H89Y	HB27+H89Y
E406W	/	Casirivimab & Imdevimab Sensitive	29.0	1.8	2.1
K417N	Beta, Gamma, Delta, Omicron	Casirivimab Resistant/Etesevimab resistant	1.6	1.3	2.6
N439K	/	Imdevimab sensitive/HB27 Epitope	1302.0	1.4	3.0
N440D	/	HB27 Epitope	49.2	3.0	12.9
N440K	Omicron	HB27 Epitope	7.3	0.9	5.2
N440Y	/	HB27 Epitope	7.7	2.2	10.4
K444N	/	Imdevimab Resistant/HB27 Epitope	2.7	1.1	1.8
K444Q	/	Imdevimab Resistant/HB27 Epitope	14.8	1.6	5.6
V445A	/	Imdevimab Resistant/HB27 Epitope	13.7	1.1	3.1
V445F	/	HB27 Epitope	6.2	1.3	3.3
G446S	Omicron	HB27 Epitope	8.0	1.8	3.1
G446V	/	Imdevimab Sensitive	117.2	2.3	7.4
Y449F	/	HB27 Epitope	28.7	1.2	1.0
Y449H	/	HB27 Epitope	3.2	1.9	4.7
L455F	/	Casirivimab Resistant	9.9	1.8	8.2
F456Y	/	RBM mutation	6.1	4.0	6.4
K458Q	/	RBM mutation	4.9	4.5	5.8
I468F	/	RBM mutation	2.6	2.8	3.4
E471Q	/	RBM mutation	7.3	3.7	6.1
I472L	/	RBM mutation	10.9	3.5	10.7
I472V	/	RBM mutation	7.8	3.0	6.8
Y473F	/	RBM mutation	8.4	2.3	8.9
A475T	/	RBM mutation	2.9	22.8	17.3
A475V	/	RBM mutation	2.9	9.7	6.8
G476A	/	H89Y Epitope	10.4	15.7	23.8
G476S	/	Casirivimab sensitive/H89Y Epitope	15.6	79.2	65.0
S477G	/	H89Y Epitope	2.3	12.3	8.6
S477I	/	H89Y Epitope	1.2	–	6.8
S477N	Omicron	H89Y Epitope	1.9	–	6.0
S477R	/	H89Y Epitope	2.4	–	4.5
T478I	/	H89Y Epitope	5.3	1.7	3.3
T478K	Delta, Omicron	H89Y Epitope	6.6	7.4	28.0
P479H	/	H89Y Epitope	4.2	390.8	8.4
P479L	/	H89Y Epitope	4.3	192.0	3.8
P479S	/	H89Y Epitope	1.7	198.6	3.3
N481K	/	RBM mutation	4.3	1.3	3.6
G482S	/	RBM mutation	3.7	1.4	1.9
E484A	Omicron	H89Y Epitope	8.4	1.9	8.0
E484K	Beta, Gamma, Mu, Iota	Bamlanivimab & Casirivimab Resistant/H89Y Epitope	6.5	3.4	6.6
E484Q	Kappa	Casirivimab sensitive/Bamlanivimab Resistant/H89Y Epitope	14.4	3.9	13.3
G485S	/	RBM mutation	5.2	2.7	6.4
F486I	/	H89Y Epitope	6.4	–	20.1
F486S	/	H89Y Epitope	10.6	1602.0	8.5
F486V	/	Casirivimab Resistant/H89Y Epitope	7.4	–	18.8
N487D	/	H89Y Epitope	26.1	14.8	58.2
Y489H	/	H89Y Epitope	7.9	32.7	26.8
F490L	/	H89Y Epitope	2.3	1.7	2.1
F490S	Lambda	Bamlanivimab Resistant/H89Y Epitope	8.4	2.0	6.2
Q493H	/	HB27 Epitope	7.8	1.6	9.9
Q493K	/	Casirivimab Resistant/HB27 Epitope	11.7	6.8	27.9
Q493L	/	HB27 Epitope	9.3	2.6	2.6
Q493R	Omicron	Bamlanivimab Resistant/HB27 Epitope	10.0	2.3	8.3
S494L	/	HB27 Epitope	4.1	1.3	0.8
S494P	/	Casirivimab sensitive/Bamlanivimab Resistant/HB27 Epitope	5.4	2.2	5.2
P499R	/	HB27 Epitope	996.9	1.6	1.4
T500S	/	HB27 Epitope	160.3	0.9	5.3
N501T	/	HB27 Epitope	1.5	1.2	1.6
N501Y	Alpha, Beta, Gamma, Mu, Omicron	HB27 Epitope	846.1	2.7	8.3
V503F	/	HB27 Epitope	12.0	3.6	4.7
Y505H	Omicron	HB27 Epitope	13.6	2.7	4.0
Y508H	/	RBM mutation	4.7	1.3	0.6

"–", the neutralizing activity of the antibody was insufficient for IC_{50} curve fitting.

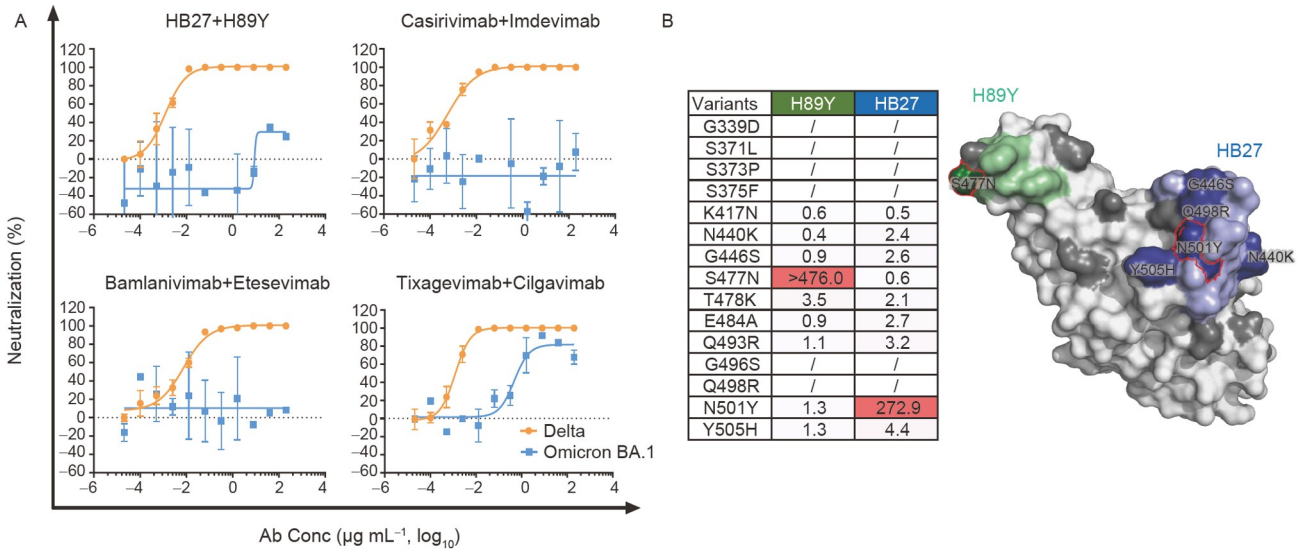

Variants	H89Y	HB27
G339D	/	/
S371L	/	/
S373P	/	/
S375F	/	/
K417N	0.6	0.5
N440K	0.4	2.4
G446S	0.9	2.6
S477N	>476.0	0.6
T478K	3.5	2.1
E484A	0.9	2.7
Q493R	1.1	3.2
G496S	/	/
Q498R	/	/
N501Y	1.3	272.9
Y505H	1.3	4.4

Figure 7 Antibody Evasion from Omicron variant BA.1. A, Neutralizing activities of the antibody cocktails against Omicron and Delta PsVs in Huh-7 cells. B, Omicron RBD mutations cause escape from HB27 and H89Y. Tables on the left exhibited the IC_{50} ratio between PsV neutralization potency against D614G and prototype strain with individual amino acid substitution in Omicron BA.1. The susceptibility reduction to individual antibody was colored in crimson. Cartoons on the right showed the RBD depicted as a white surface with the antibodies H89Y epitope in cyan, and antibodies HB27 epitope in wathet. The superposition between amino acid substitutions in Omicron BA.1 and antibody epitopes were depicted as dark green and navy blue for the two individual antibody of the cocktail, respectively, and the rest amino acid substitutions within Omicron BA.1 RBD were labeled in dark grey. Key amino acid substitutions with reduced susceptibility to individual antibodies were circled red line onto the structure of the RBD. "/", not detected.

tralization experiments against a panel of pseudoviruses with single amino acid substitution within Omicron RBD that overlapped with critical binding sites for both HB27 and H89Y (Figure 7, Table 3). However, the escape mutation screening experiment results indicated that the antibody cocktail efficiently prevented incidence of any escape mutations. The "contradictory" results were most likely due to the limitation of virus mutant frequency after two rounds of passages *in vitro* compared with that of authentic virus in real world, which is under the pressure of multiple neutralizing antibodies with different RBD binding epitopes, resulting in Omicron harboring strikingly accumulated mutations in RBD. In order to fully understand cocktail and individual antibodies effectiveness, additional studies on neutralizing activities against pseudoviruses with mutation sites in pandemic variants are supplied to bridge this important knowledge gap.

Besides HB27+H89Y cocktail, the two EUA antibody cocktails, Casirivimab+Imdevimab and Bamlanivimab +Etesevimab completely lost neutralizing activity to Omicron variant as well (Figure 7). Omicron was fully resistant against these cocktails mediated neutralization because K417N, N440K, G446S, S477N, T478K, E484A, Q493R, G496S, Q498R, N501Y, and Y505H mutations in RBD are located within or close to the epitopes bound by these antibodies (Hoffmann et al., 2022) (Figure 2). Casirivimab activity was affected by K417N and E484A as a result of the loss of hydrogen bond interactions (Tada et al., 2022). Imdevimab activity was affected by N440K and G446S as these mutations will introduce steric hindrance (Dejnirattisai et al., 2022a; Li et al., 2022). The activities of both Etesevimab and Bamlanivimab were affected by Q493R which will lead to the loss of hydrogen bond interactions or the collision between antibody and Omicron (Li et al., 2022). Besides, Tixagevimab+Cilgavimab cocktail retained modest neutralizing activity against Omicron as they only moderately influenced by E484A and Q498R (Tixagevimab) or G446V and E484A (Cilgavimab), since these residues are only located on the fringe of the epitopes of Tixagevimab and Cilgavimab (Tada et al., 2022). These evidences are possible explanations why Omicron variant is able to escape from current antibody treatments.

Our results highlighted the advantages of HB27+H89Y cocktail over its two single antibody components in terms of IC_{50} values and breadth of neutralization spectrum. The cocktail binds to epitopes different from that of three EUA antibody cocktails, and also showed different mutational resistant profiles. The breadth of the HB27+H89Y cocktail in neutralizing SARS-CoV-2 variants was not sufficient to cover the newly emerged Omicron variants, therefore efforts to search for new antibody cocktails capable of binding to more conserved epitopes are warranted.

MATERIALS AND METHODS

Cells and viruses

Human embryonic kidney 293T cell line (Cat: CRL-11268)

used for pseudovirus packaging was purchased from ATCC. Vero-E6 cells were purchased from Chinese Academy of Medical Sciences Cell Bank (Cat: GN017). Huh-7 cells were purchased from China Center for Type Culture Collection. Vero cells, 293T, Huh-7 cells and Vero-E6 cells were grown in Dulbecco's modified Eagle's medium (DMEM) containing 10% (*v*/*v*) fetal bovine serum (FBS). The sequence of SARS-CoV-2 BetaCoV/Beijing/IMEBJ01/2020 viral strain was identical to Wuhan strain. Beta (CSTR.16698.06.NPRC 2.062100001) and Delta (CSTR.16698.06.NPRC 6.CCPM-B-V-049-2105-6) variants were from Beijing Institute of Microbiology and Epidemiology. The virus was amplified and titrated by standard plaque forming assay using Vero cells. The stock solution of the virus was 6×10^5, 1.5×10^5 and 2.0×10^6 $CCID_{50}$ (cell culture infectious dose 50%) mL^{-1}, respectively.

Reagents, recombinant proteins and antibodies

Recombinant spike protein (Cat: 40589-V08B1 and Cat: 40592-V05H), recombinant RBD protein of SARS-CoV-2 (Cat: 40592-V08H), recombinant ACE2 protein (Cat: 10108-H02H and Cat: 10108-H08H), transfection reagent Sinofection (Cat: STF02), mammalian expression plasmids of full length spike or RBD protein of SARS-CoV-2 (Cat: VG40589-UT, Wuhan/IVDC-HB-01/2019), were purchased from Sino Biological. Fetal bovine serum (FBS) (Cat: 10091148) was purchased from Life Technologies. Hygromycin (Cat: V900372) was purchased from Sigma-Aldrich. Luciferase assay system (Cat: E1501) and Passive Lysis 5× buffer (E1941) were purchased from Promega. Anti-human IgG Fc/HRP (Cat: 5210-0165) were purchased from KPL. Goat anti-human IgG F(ab')2/HRP (Cat: 109-036-006) were purchased from Jackson ImmunoResearch. Lip 2000(11668-019) was purchased from Invitrogen. Avidin (Cat: A9275-25MG) was purchase from Sigma-Aldrich Merck.

Generation of antibodies

Antibodies were generated as previously described (Zhu et al., 2021). Briefly, antibodies against SARS-CoV-2 were screened from phage-display single-chain fragment variable (scFv) libraries constructed from spleen mRNA of BALB/c mice immunized with recombinant SARS-CoV-2 RBD. The recombinant SARS-CoV-2 RBD was used as bait protein to select for specific anti-RBD scFvs via bio panning. Phages of ACE2-RBD interaction blocking and non-competitive binding of HB27 to RBD were further selected. Candidate scFvs with potent binding for recombinant SARS-CoV-2 RBD were further generated with human IgG1 Fc with Leu234Ala and Leu235Ala (LALA) mutation. Antibodies were expressed using CHO transfection production system. Imdevimab and Casirivimab (PDB: 6XDG), Bamlanivimab and Etesevimab cocktail (PDB: 7KMG and 7C01) and Tixagevimab and Cilgavimab cocktail (PDB: 7L7E) were produced in HEK293 based on the sequences from PDB.

Animals

Aged BALB/c mice at 7–8 months of age were purchased from National Institute for Food and Drug Control (NICPBP, Beijing, China). The animals were housed in a specific pathogen-free facility until they were transferred into a biosafety level 3 (BSL-3) animal facility for virus challenge.

Expression of recombinant RBD proteins with single site mutation

Several surface exposed sites in the SARS-CoV-2 RBD (residues 319-541, GenBank: MN908947.3), were selected, and the amino acid was mutated to another type with different characteristics (e.g., Glu was mutated to Arg). These selected sites were distributed over the whole surface of the SARS-CoV2 RBD. Mutated RBD genes with His-tag were cloned into pSTEP2 vector and transfected into HEK293E cells for protein expression. Supernatants were collected and purified using immobilized metal-ion affinity chromatography (IMAC) resins.

Enzyme-linked immunosorbent assay

Recombinant RBD protein of SARS-CoV-2 was coated on 96 well plates using CBS buffer over night at 4°C. BSA was used for blocking at room temperature for 1 h. Indicated corresponding proteins or antibodies were then added and incubated at room temperature for 1 h. After washing the unbound proteins or antibodies away, secondary antibody with horseradish peroxidase (HRP) labelling was added and incubated for another 1 h. Developing buffer was added and incubated for 5–30 min, 1% H_2SO_4 was added to stop the reaction, and absorbance at 450 nm was detected with a microplate reader.

Epitope mapping of antibodies by ELISA

Epitope of antibodies was mapped using various recombinant SARS-CoV-2 RBD proteins carrying different site mutations by ELISA following the protocol mentioned above. Mutations that led to over 50% decrease in binding compared with the wild type protein were defined as critical binding sites for specific antibody.

Protein biotinylation

Recombinant proteins were biotinlyated using EZ-Link NHS-Biotin Reagents from Thermo Scientific (21343). In a

nutshell, proteins were exchanged into an amine-free buffer such as PBS and 1 mg mL^{-1} of biotin was added and incubated at room temperature for 30 min. Protein solution was then dialyzed to remove non-reacted biotin. The concentration of biotinylated protein was determined using ultraviolet (UV) spectrometry.

Affinity measurement by Bio-layer Interferometry assay

Recombinant SARS-CoV-2 RBD or spike protein was biotinylated and loaded using SA sensor (Pall Corporation). HB27, H89Y or antibody cocktail were added for real-time association and dissociation analysis using Octet system. For analysis of competition between HB27 and H89Y for RBD or spike binding, recombinant SARS-CoV-2 RBD or spike protein was biotinylated and loaded using streptavidin (SA) sensor, one antibody was added first for 600 s, another indicated antibody was loaded afterwards. Data Analysis Octet was used for data processing.

Pseudovirus production in 293T adherent cells

Pseudoviruses were replication-deficient vesicular stomatitis virus (VSV) with its VSV-G protein gene replaced by a luciferase reporter gene in the genome. Constructions of these pseudoviruses were described previously (Fukushi et al., 2008; Whitt, 2010). Briefly, expression vector pCMV3-2019-nCoV-spike encoding spike protein of Wuhan-Hu-1 strain (GISAID accession: EPI_ISL_402125) or vector of variants were transfected into 293T cells and cultured in CO_2 incubator for 16–24 h. VSV-G was added into the above cell supernatant by a certain multiplicity of infection (MOI). After infection of cells, supernatant was discarded and cells were washed to remove the uninfected virus. Fresh medium was added for further culture. 24–48 h after infection, virus was collected and filtered to discard cell debris. Accession IDs of VOC/VOIs: D614G (EPI_ISL_406862), B.1.1.7 (EPI_ISL_764238), B.1.351 (EPI_ISL_736940), P.1 (EPI_ISL_792680), B.1.617.2 (EPI_ISL_1999775), BA.1 (EPI_ISL_6640917), C.37 (EPI_ISL_2756117), B.1.621 (EPI_ISL_3856732), B.1.526 (EPI_ISL_1588435), B.1.429 (EPI_ISL_730092), B.1.617.1 (EPI_ISL_1704611).

Pseudovirus neutralization assay

Huh-7 cells were seeded in 96 well plates at 30,000 cells $well^{-1}$. 200 $TCID_{50}$/25 μL pseudovirus were incubated with indicated antibodies or serum at 37°C in 5% CO_2 incubator for 1 h and added to seeded cells and incubated at 37°C CO_2 incubator for 24 h. Positive control was set up as adding 200 $TCID_{50}$/25μL pseudovirus into cells, blank was described as only adding complete growth medium into cells. Luciferase luminescence relative light unit (RLU) was then measured using luciferase assay system. Neutralization percentage was calculated as: Inhibition%=100%–(Sample RLU–Blank RLU)/(Positive RLU–Blank RLU). Antibodies neutralization titers were presented as half effective neutralizing concentration (IC_{50}).

ACE2-competitive ELISA assay

Recombinant ACE2-Fc protein of 4 μg mL^{-1} was coated on 96 well plate, 100 μL per well at 2–8°C overnight. The plates were washed and blocked over 1 h at room temperature the next day. Biotinylated S-Trimer (100 ng mL^{-1}) mixed with different antibody or serum were added to plates and incubated for 1 h. After washing three times with TBST, 0.2 μg mL^{-1} of Streptavidin-HRP was then added for detection after several washes. Microplate reader was used to detect A_{450} after reaction stopped. Inhibition PI%=(A_{Blank}–A_{Sample})/A_{Blank}×100%, among which A_{Blank} means the group with S-Trimer but no antibody or serum, while A_{Sample} means the group with both S-Trimer and antibody/serum at a given dilution. GraphPad Prism8.0 was used to fit the S-curve and analyze the ability of the antibody/serum to compete for the binding of S-Trimer to ACE2 receptor, draw a dose-effect curve (antibody concentration as the x axis and A_{450} as the y axis) and calculate the IC_{50} value.

Micro-neutralizing test (MNT)

50 μL antibodies of gradient dilution was mixed with equal volume of 100 $CCID_{50}$ virus. Virus control and normal cell control were set up and all groups were incubated at 37°C for 1 h. 100 μL, 1.5×10^5 cells mL^{-1} Vero cell suspension was added to each well and incubated at 37°C for 3–5 days. The neutralizing activity of antibody against SARS-CoV-2 virus was determined by cytopathic effect (CPE) and calculated by Karber method, as IC_{50} of the antibody corresponding to the maximum dilution ratio that can protect 50% of cells from 100 $CCID_{50}$ virus.

Antibody escape mutation screening

Antibody escape mutation screening was conducted as reported previously (Baum et al., 2020). The selection agent is a replication-competent recombinant VSV carrying eGFP reporter named rVSV-eGFP-SARS-CoV-2, which expresses SARS-CoV-2 Wuhan-Hu-1 strain spike protein (GeneBank: YP_009724390.1) in replacement of the original VSV G (Li et al., 2020; Li et al., 2021a). Briefly, Vero cells were seeded in 12-well plate at 2×10^5 cells per well. The next day, antibodies were 5-fold serially diluted starting from 100 μg mL^{-1} into 11 subsequent gradient concentrations. Negative control without antibody was also included. Five hundred microliter

of rVSV-eGFP-SARS-CoV-2 (1×10^6 focus-forming units, FFU mL^{-1}) was mixed with equal volume of the antibody diluent, and incubated at room temperature for 30 min. After incubation, the mixture was added to the monolayer of Vero cells in the 12-well plate and incubated in a 37°C, 5% CO_2 incubator for 96 h. The supernatants from the wells with the highest antibody dilution that showed extensive GFP foci were collected and used for the second round of screening. Viral RNAs were extracted from the supernatants of passage 1 and 2 (P1 and P2) for next generation sequencing to analyze the escape mutations of S protein.

Mouse protection efficacy

Aged BALB/c mice were intranasally challenged with 4×10^5 PFU mL^{-1} SARS-CoV-2 Beta variant (CSTR.16698.06.NPRC2.062100001) (Chen et al., 2022; Gu et al., 2020). Mice were randomized into 4 groups (due to the limitation of BSL-3 facilities, mice were not evenly distributed: 4 in PBS control group, 3 in 400 μg HB27 monotherapy group, 3 in 400 μg H89Y monotherapy group and 5 in 400 μg HB27 and 400 μg H89Y cocktail group. Four hours after virus inoculation, mice were injected intravenously with vehicle PBS or antibodies. At five days post virus infection, the mice were euthanized. Their lung tissues were dissected for RNA extraction and histological analysis. One lobe of each lung tissue was homogenized in AVL buffer to extract RNAs and the remaining part of the lung was fixed with 4% paraformaldehyde (PFA) for H & E staining.

Viral nucleic acid extraction

Total viral RNA was extracted using QIAampViral RNA Mini Kit (QIAGEN), according to the manufacturer's protocol. Briefly, the tissue homogenates were mixed with AVL buffer and homogenized with stainless steel beads in a Tissuelyser-24 (Shanghai Jingxin Industrial Development) in 1 mL of DMEM and centrifuged. The supernatants were mixed with 560 μL of absolute ethanol and centrifuged. The supernatants were loaded on the unsoaked QIAamp column, centrifuged at 8,000 r min^{-1} for 1 min, washed with AW1 buffer and AW2 buffer, followed by centrifuging. The bound RNAs were eluted with 60 μL of AVE elution buffer and centrifuged at 8000 r min^{-1} for 1 min. The eluents containing viral RNA were tested immediately or stored below –80°C.

Quantitative real-time polymerase chain reaction (qRT-PCR)

Viral RNAs in the lung tissues from the virus-infected mice were analyzed by qRT-PCR. Briefly, the extracted SARS-CoV-2 RNAs were reversely transcribed into cDNAs at 42°C for 5 min using One Step PrimeScript RT-PCR Kit (TaKaRa) and PCR-amplified using the SARS-CoV-2 specific primers and probes: sgRNA-F (5′-CGATCTCTTGTAGATCT-GTTCTC-3′), sgRNA-R (5′-ATATTGCAGCAGTACGCA-CACA-3'), and sgRNA-P3 (5′- FAM-ACACTAGC-CATCCTTACTGCGCTTCG-BHQ1-3′). The PCR reactions were performed in duplicate at 95°C for 10 s; and subjected to 40 cycles of 95°C for 5 s, 60°C for 20 s. The virus loads were determined, according to the standard curve established by serial ten-fold dilutions of SARS-CoV-2 RNA.

Hematoxylin and eosin (H & E) staining

The collected lung tissues were fixed in 4% paraformaldehyde and paraffin-embedded. The tissue sections (3 μm) were dewaxed, rehydrated and regularly stained with H & E. Images were recorded using Olympus BX51 microscope equipped with a DP72 camera.

NGS sequencing

Next-Generation Sequencing (NGS) analysis was perform using Array Studio software package platform (Omicsoft). Quality of paired-end RNA Illumina reads was assessed using the "raw data QC of RNA-Seq data suite". Minimum and maximum read length, total nucleotide number, and GC % were calculated.

Statistical analysis

Comparisons among treatment groups and control group were conducted with unpaired, two tailed *t*-test or Mann-Whitney tests in virus challenging study using GraphPad Prism 8. *P*-value of *<0.05 was considered statistically significant.

Compliance and ethics

L.X. and C.S. are listed as inventors on pending patent applications for HB27 and HB27+H89Y cocktail. C.S., J.L., J.Y., F.W., L.S., Y.Z., P.H., and L.X. are employed by and have ownership or potential stock option in Sinocelltech Group Limited. No other competing interests were declared by the authors.

Experiments involving authentic SARS-CoV-2 virus were performed in the biosafety level 3 (P3+) facilities in the Institute of Microbiology and Epidemiology, Academy of Military Medical Sciences. Animal experiments were approved by the Animal Experiment Committee of Laboratory Animal Center, Beijing Institute of Microbiology and Epidemiology (approval number: IACUC-DWZX-2020-002). All applicable institutional and/or national guidelines for the care and use of animals were followed.

Compliance and ethics *The author(s) declare that they have no conflict of interest.*

Acknowledgements *This work was supported by the National Key Research and Development Project of China (2021YEF0201700).*

References

Andrews, N., Stowe, J., Kirsebom, F., Toffa, S., Rickeard, T., Gallagher, E., Gower, C., Kall, M., Groves, N., O'Connell, A.M., et al. (2022). Covid-19 vaccine effectiveness against the Omicron (B.1.1.529) variant. N Engl J Med 386, 1532–1546.

Baum, A., Fulton, B.O., Wloga, E., Copin, R., Pascal, K.E., Russo, V., Giordano, S., Lanza, K., Negron, N., Ni, M., et al. (2020). Antibody cocktail to SARS-CoV-2 spike protein prevents rapid mutational escape seen with individual antibodies. Science 369, 1014–1018.

Burki, T.K. (2021). Lifting of COVID-19 restrictions in the UK and the Delta variant. Lancet Respir Med 9, e85.

Cao, Y., Wang, J., Jian, F., Xiao, T., Song, W., Yisimayi, A., Huang, W., Li, Q., Wang, P., An, R., et al. (2022a). Omicron escapes the majority of existing SARS-CoV-2 neutralizing antibodies. Nature 602, 657–663.

Cao, Y., Wang, X., Li, S., Dong, Y., Liu, Y., Li, J., Zhao, Y., and Feng, Y. (2022b). A third high dose of inactivated COVID-19 vaccine induces higher neutralizing antibodies in humans against the Delta and Omicron variants: a randomized, double-blinded clinical trial. Sci China Life Sci 65, 1677–1679.

Chen, J., Wang, R., Wang, M., and Wei, G.W. (2020). Mutations strengthened SARS-CoV-2 infectivity. J Mol Biol 432, 5212–5226.

Chen, Q., Huang, X.Y., Liu, Y., Sun, M.X., Ji, B., Zhou, C., Chi, H., Zhang, R.R., Luo, D., Tian, Y., et al. (2022). Comparative characterization of SARS-CoV-2 variants of concern and mouse-adapted strains in mice. J Med Virol 94, 3223–3232.

Corti, D., Purcell, L.A., Snell, G., and Veesler, D. (2021). Tackling COVID-19 with neutralizing monoclonal antibodies. Cell 184, 3086–3108.

Dejnirattisai, W., Huo, J., Zhou, D., Zahradník, J., Supasa, P., Liu, C., Duyvesteyn, H.M.E., Ginn, H.M., Mentzer, A.J., Tuekprakhon, A., et al. (2022a). SARS-CoV-2 Omicron-B.1.1.529 leads to widespread escape from neutralizing antibody responses. Cell 185, 467–484.e15.

Dejnirattisai, W., Shaw, R. H., Supasa, P., Liu, C., Stuart, A. S., Pollard, A. J., Liu, X., Lambe, T., Crook, D., Stuart, D. I., et al. (2022b). Reduced neutralisation of SARS-CoV-2 omicron B.1.1.529 variant by post-immunisation serum. Lancet 399, 234–236.

Deng, X., Garcia-Knight, M.A., Khalid, M.M., Servellita, V., Wang, C., Morris, M.K., Sotomayor-González, A., Glasner, D.R., Reyes, K.R., Gliwa, A.S., et al. (2021). Transmission, infectivity, and neutralization of a spike L452R SARS-CoV-2 variant. Cell 184, 3426–3437.e8.

Du, L., Yang, Y., and Zhang, X. (2021). Neutralizing antibodies for the prevention and treatment of COVID-19. Cell Mol Immunol 18, 2293–2306.

FDA. (2020). Emergency Use Authorization (EUA) for Bamlanivimab 700 mg and Etesevimab 1400 mg IV Administered Together Center for Drug Evaluation and Research (CDER) Review. U.S. Food & Drug Administration.

FDA. (2022a). Fact sheet for health care providers emergency use authorization (EUA) of Regen-Cov®(casirivimab and imdevimab), U.S. Food and Drug Administration.

FDA. (2022b). Fact sheet for health care providers emergency use authorization (EUA) of bamlanivimab and etesevimab, U.S. Food and Drug Administration.

Fukushi, S., Watanabe, R. and Taguchi, F. (2008). Pseudotyped vesicular stomatitis virus for analysis of virus entry mediated by SARS coronavirus spike proteins. Methods Mol Biol (Clifton, N.J.) 454, 331–338.

Gu, H., Chen, Q., Yang, G., He, L., Fan, H., Deng, Y.Q., Wang, Y., Teng, Y., Zhao, Z., Cui, Y., et al. (2020). Adaptation of SARS-CoV-2 in BALB/c mice for testing vaccine efficacy. Science 369, 1603–1607.

Hansen, J., Baum, A., Pascal, K.E., Russo, V., Giordano, S., Wloga, E., Fulton, B.O., Yan, Y., Koon, K., Patel, K., et al. (2020). Studies in humanized mice and convalescent humans yield a SARS-CoV-2 antibody cocktail. Science 369, 1010–1014.

Hoffmann, M., Krüger, N., Schulz, S., Cossmann, A., Rocha, C., Kempf, A., Nehlmeier, I., Graichen, L., Moldenhauer, A.S., Winkler, M.S., et al. (2022). The Omicron variant is highly resistant against antibody-mediated neutralization: implications for control of the COVID-19 pandemic. Cell 185, 447–456.e11.

Jones, B.E., Brown-Augsburger, P.L., Corbett, K.S., Westendorf, K., Davies, J., Cujec, T.P., Wiethoff, C.M., Blackbourne, J.L., Heinz, B.A., Foster, D., et al. (2021). The neutralizing antibody, LY-CoV555, protects against SARS-CoV-2 infection in nonhuman primates. Sci Transl Med 13, eabf1906.

Li, H., Zhang, Y., Li, D., Deng, Y.Q., Xu, H., Zhao, C., Liu, J., Wen, D., Zhao, J., Li, Y., et al. (2021a). Enhanced protective immunity against SARS-CoV-2 elicited by a VSV vector expressing a chimeric spike protein. Sig Transduct Target Ther 6, 389.

Li, H., Zhao, C., Zhang, Y., Yuan, F., Zhang, Q., Shi, X., Zhang, L., Qin, C., and Zheng, A. (2020). Establishment of replication-competent vesicular stomatitis virus-based recombinant viruses suitable for SARS-CoV-2 entry and neutralization assays. Emerging Microbes Infects 9, 2269–2277.

Li, M., Lou, F., and Fan, H. (2022). SARS-CoV-2 variant Omicron: currently the most complete "escapee" from neutralization by antibodies and vaccines. Sig Transduct Target Ther 7, 28.

Li, Y., Qi, L., Bai, H., Sun, C., Xu, S., Wang, Y., Han, C., Li, Y., Liu, L., Cheng, X., et al. (2021b). Safety, tolerability, pharmacokinetics, and immunogenicity of a monoclonal antibody (SCTA01) targeting SARS-CoV-2 in healthy adults: a randomized, double-blind, placebo-controlled, phase I study. Antimicrob Agents Chemother 65, e0106321.

Liang, K.H., Chiang, P.Y., Ko, S.H., Chou, Y.C., Lu, R.M., Lin, H.T., Chen, W.Y., Lin, Y.L., Tao, M.H., Jan, J.T., et al. (2021). Antibody cocktail effective against variants of SARS-CoV-2. J Biomed Sci 28, 80.

Liu, L., Iketani, S., Guo, Y., Chan, J.F.W., Wang, M., Liu, L., Luo, Y., Chu, H., Huang, Y., Nair, M.S., et al. (2022). Striking antibody evasion manifested by the Omicron variant of SARS-CoV-2. Nature 602, 676–681.

Liu, Q., Qin, C., Liu, M., and Liu, J. (2021). Effectiveness and safety of SARS-CoV-2 vaccine in real-world studies: a systematic review and meta-analysis. Infect Dis Poverty 10, 132.

Liu, Y., Liu, J., Plante, K. S., Plante, J. A., Xie, X., Zhang, X., Ku, Z., An, Z., Scharton, D., Schindewolf, C., et al. (2021). The N501Y spike substitution enhances SARS-CoV-2 transmission. bioRxiv, 2021.2003.2008.434499.

Lu, L., Zhang, H., Zhan, M., Jiang, J., Yin, H., Dauphars, D.J., Li, S.Y., Li, Y., and He, Y.W. (2020). Antibody response and therapy in COVID-19 patients: what can be learned for vaccine development? Sci China Life Sci 63, 1833–1849.

Piccoli, L., Park, Y.J., Tortorici, M.A., Czudnochowski, N., Walls, A.C., Beltramello, M., Silacci-Fregni, C., Pinto, D., Rosen, L.E., Bowen, J.E., et al. (2020). Mapping Neutralizing and Immunodominant sites on the SARS-CoV-2 spike receptor-binding domain by structure-guided high-resolution serology. Cell 183, 1024–1042.e21.

Pinto, D., Park, Y.J., Beltramello, M., Walls, A.C., Tortorici, M.A., Bianchi, S., Jaconi, S., Culap, K., Zatta, F., De Marco, A., et al. (2020). Cross-neutralization of SARS-CoV-2 by a human monoclonal SARS-CoV antibody. Nature 583, 290–295.

Plante, J.A., Liu, Y., Liu, J., Xia, H., Johnson, B.A., Lokugamage, K.G., Zhang, X., Muruato, A.E., Zou, J., Fontes-Garfias, C.R., et al. (2021). Spike mutation D614G alters SARS-CoV-2 fitness. Nature 592, 116–121.

Sadoff, J., Le Gars, M., Cardenas, V., Shukarev, G., Vaissiere, N., Heerwegh, D., Truyers, C., de Groot, A. M., Scheper, G., Hendriks, J., et al. (2021). Durability of antibody responses elicited by a single dose of

Ad26.COV2.S and substantial increase following late boosting. medRxiv, 2021.2008.2025.21262569.
Shi, R., Shan, C., Duan, X., Chen, Z., Liu, P., Song, J., Song, T., Bi, X., Han, C., Wu, L., et al. (2020). A human neutralizing antibody targets the receptor-binding site of SARS-CoV-2. Nature 584, 120–124.
Starr, T.N., Greaney, A.J., Addetia, A., Hannon, W.W., Choudhary, M.C., Dingens, A.S., Li, J.Z., and Bloom, J.D. (2021). Prospective mapping of viral mutations that escape antibodies used to treat COVID-19. Science 371, 850–854.
Tada, T., Zhou, H., Dcosta, B. M., Samanovic, M. I., Chivukula, V., Herati, R. S., Hubbard, S. R., Mulligan, M. J. and Landau, N. R. (2022). Increased resistance of SARS-CoV-2 Omicron variant to neutralization by vaccine-elicited and therapeutic antibodies. eBioMedicine 78.
Takashita, E., Kinoshita, N., Yamayoshi, S., Sakai-Tagawa, Y., Fujisaki, S., Ito, M., Iwatsuki-Horimoto, K., Chiba, S., Halfmann, P., Nagai, H., et al. (2022a). Efficacy of antibodies and antiviral drugs against COVID-19 omicron variant. N Engl J Med 386, 995–998.
Takashita, E., Kinoshita, N., Yamayoshi, S., Sakai-Tagawa, Y., Fujisaki, S., Ito, M., Iwatsuki-Horimoto, K., Halfmann, P., Watanabe, S., Maeda, K., et al. (2022b). Efficacy of antiviral agents against the SARS-CoV-2 omicron subvariant BA.2. N Engl J Med 386, 1475–1477.
Tao, K., Tzou, P.L., Nouhin, J., Gupta, R.K., de Oliveira, T., Kosakovsky Pond, S.L., Fera, D., and Shafer, R.W. (2021). The biological and clinical significance of emerging SARS-CoV-2 variants. Nat Rev Genet 22, 757–773.
Tseng, H.F., Ackerson, B.K., Luo, Y., Sy, L.S., Talarico, C.A., Tian, Y., Bruxvoort, K.J., Tubert, J.E., Florea, A., Ku, J.H., et al. (2022). Effectiveness of mRNA-1273 against SARS-CoV-2 Omicron and Delta variants. Nat Med 28, 1063–1071.
Weisblum, Y., Schmidt, F., Zhang, F., DaSilva, J., Poston, D., Lorenzi, J.C., Muecksch, F., Rutkowska, M., Hoffmann, H.H., Michailidis, E., et al. (2020). Escape from neutralizing antibodies by SARS-CoV-2 spike protein variants. eLife 9, e61312.
Whitt, M.A. (2010). Generation of VSV pseudotypes using recombinant ΔG-VSV for studies on virus entry, identification of entry inhibitors, and immune responses to vaccines. J Virol Methods 169, 365–374.
WHO. (2022). WHO Coronavirus (COVID-19). Dashboard, World Health Organization.
Zhou, B., Zhou, R., Chan, J. F.-W., Luo, M., Peng, Q., Yuan, S., Mok, B. W.-Y., Chen, B., Wang, P., Poon, V. K.-M., et al. (2022). An elite broadly neutralizing antibody protects SARS-CoV-2 Omicron variant challenge. bioRxiv, 2022.2001.2005.475037.
Zhu, L., Deng, Y.Q., Zhang, R.R., Cui, Z., Sun, C.Y., Fan, C.F., Xing, X., Huang, W., Chen, Q., Zhang, N.N., et al. (2021). Double lock of a potent human therapeutic monoclonal antibody against SARS-CoV-2. Natl Sci Rev 8, nwaa297.
Zost, S.J., Gilchuk, P., Case, J.B., Binshtein, E., Chen, R.E., Nkolola, J.P., Schäfer, A., Reidy, J.X., Trivette, A., Nargi, R.S., et al. (2020). Potently neutralizing and protective human antibodies against SARS-CoV-2. Nature 584, 443–449.

SUPPORTING INFORMATION

The supporting information is available online at https://doi.org/10.1007/s11427-022-2166-y. The supporting materials are published as submitted, without typesetting or editing. The responsibility for scientific accuracy and content remains entirely with the authors.